Supporting Information

Figure 1s Changes in the UV–Vis absorption spectra by titration of **[Zn(L^1)(Py)]** with $Nd(NO_3)_3$•6(H_2O) in MeCN solutions (4×10^{-5} M)

Figure 2s Titration of **[Zn(L^1)(Py)]** with $Nd(NO_3)_3$•6(H_2O) in MeCN solution (4×10^{-5} M), showing the quenching of **[Zn(L^1)(Py)]** chromophore-based visible emission upon gradual addition of $Nd(NO_3)_3$•6(H_2O)

Figure 3s Titration of **[Zn(L^1)(Py)]** with $Nd(NO_3)_3$•6(H_2O) in MeCN solution (4×10^{-5} M), showing a gradual increase of Nd-centered NIR emission upon gradual addition of $Nd(NO_3)_3$•6(H_2O)

Figure 4s Changes in the UV–Vis absorption spectra by titration of **[Zn(L^2)(Py)]** with $Nd(NO_3)_3$•6(H_2O) in MeCN solutions (4×10^{-5} M)

Figure 5s Titration of **[Zn(L^2)(Py)]** with $Nd(NO_3)_3$•6(H_2O) in MeCN solutions (4×10^{-5} M), showing the gradual quenching of **[Zn(L^2)(Py)]** chromophore-based visible emission upon gradual addition of $Nd(NO_3)_3$•6(H_2O)

Figure 6s Titration of **[Zn(L^2)(Py)]** with $Nd(NO_3)_3$•6(H_2O) in MeCN solutions (4×10^{-5} M), showing a gradual increase of Nd-centered NIR emission upon gradual addition of

$Nd(NO_3)_3 \cdot 6(H_2O)$

Figure 1s

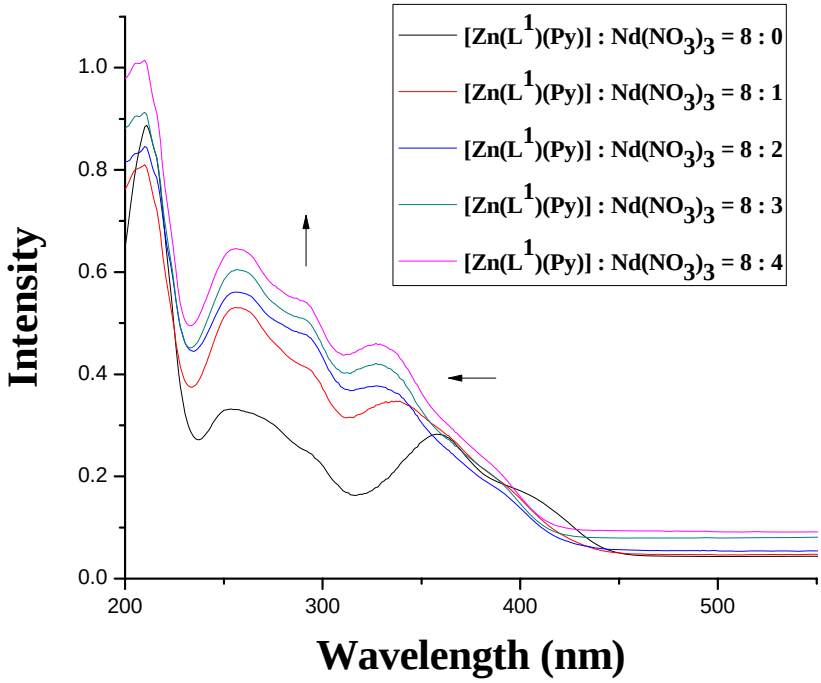

Figure 2s

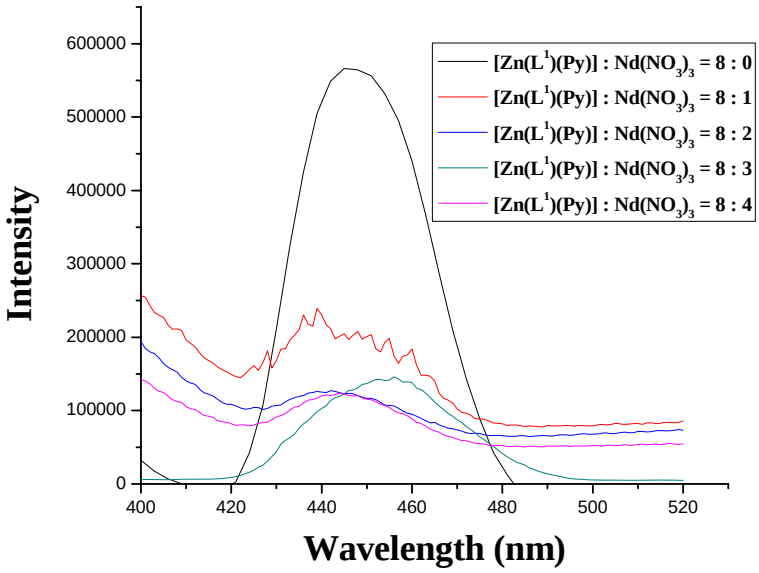

Figure 3s

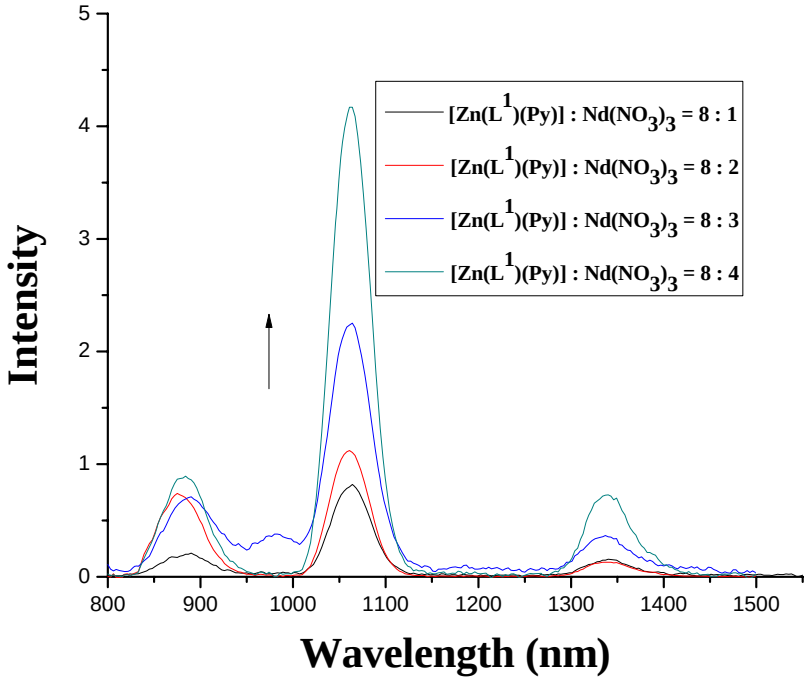

Figure 4s

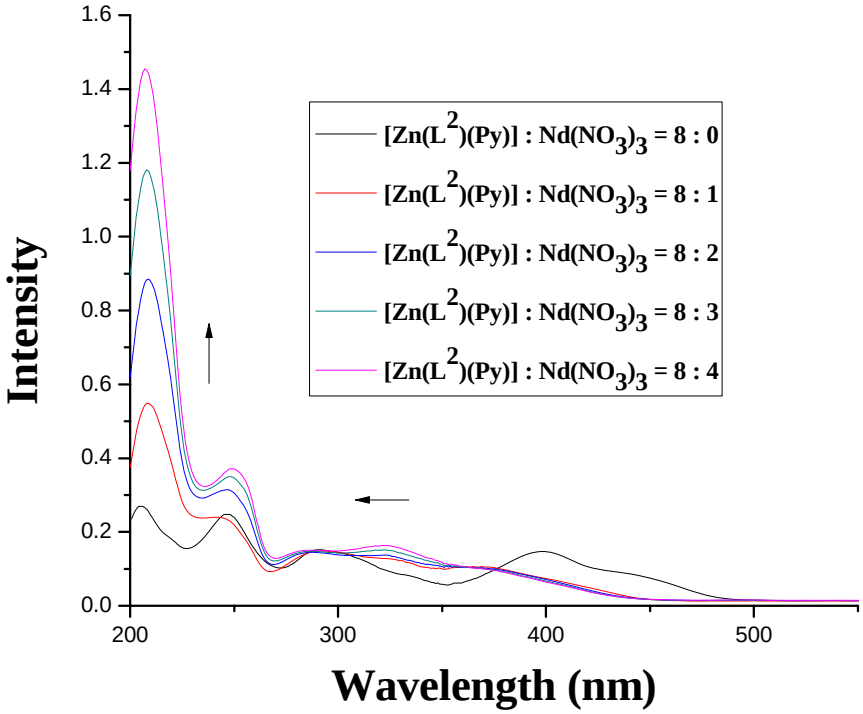

Figure 5s

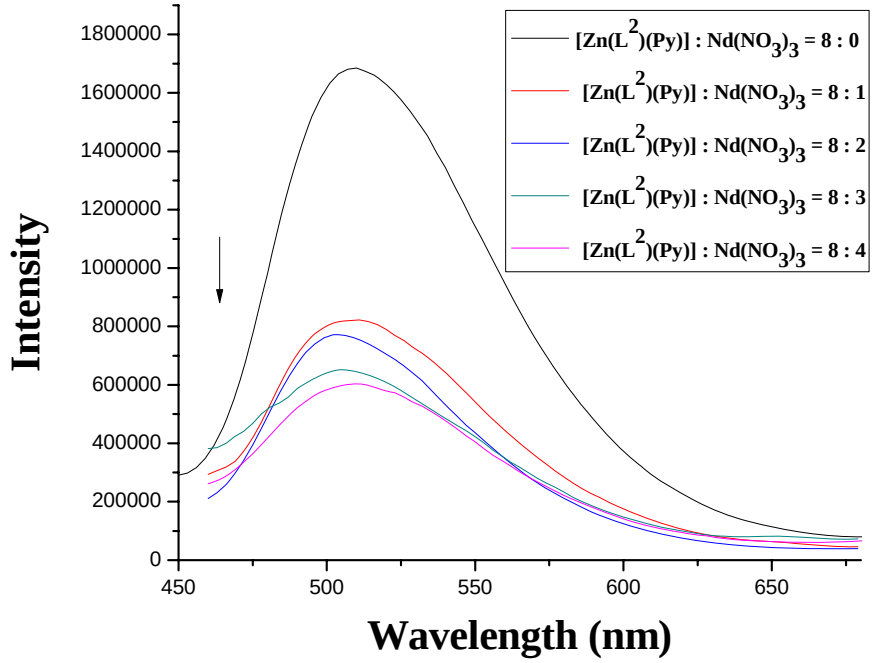

Figure 6s